Edelweiss Applied Science and Technology
ISSN: 2576-8484
Vol. 10, No. 1, 1-15
2026
Publisher: Learning Gate
DOI: 10.55214/2576-8484.v10i1.11489

Identification of adulterated white pepper powder with roasted rice by using near-infrared hyperspectral imaging

Saranya Workhwa[1], Janejira Jamjuree[2], Chutikan Opatworakitkun[2], Chutima Rungsawang[2], Woranitta Sahachairungrueng[1], Anthony Keith Thompson[3], Sontisuk Teerachaichayut[2*]
[1]Department of Food Science, School of Food-Industry, King Mongkut's Institute of Technology, Ladkrabang, Bangkok 10520, Thailand; saranyaworkhwa@gmail.com (S.W.), woranitta.s@gmail.com (W.S.).
[2]Department of Food Process Engineering, School of Food-Industry, King Mongkut's Institute of Technology, Ladkrabang, Bangkok10520, Thailand; kujanejub@gmail.com (J.J.); Chutikanpp31@gmail.com (C.O.), chutima050644@gmail.com (C.R.), sontisuk.te@kmitl.ac.th (S.T.).
[3]Department of Postharvest Technology, Cranfield University, College Road, Cranfield, Bedford, MK43 0AL, United Kingdom; keiththompson28@yahoo.com (A.K.T.).

Abstract: The substitution of powdered white pepper on the commercial market with similar, but cheaper powders extracted from various food products can make it more profitable, but reduce its quality. Near-infrared hyperspectral imaging (NIR-HSI) is a technique that has been successfully used to detect contamination in other food products. Therefore, NIR-HSI was tested on powdered white pepper that had been adulterated with various levels of roasted rice powder, using partial least squares discriminant analysis (PLS-DA), support vector machine classification (SVMC), partial least squares regression (PLSR), and support vector machine regression (SVMR) methods to test whether adulteration could be detected, and if so, at what level. The results showed that the highest predictive accuracy of classification was 100% by using PLS-DA. The calibration model was also developed to determine the level of adulteration in white pepper powder by roasted rice powder. The SVMR model gave the highest predictive accuracy with a coefficient of determination for prediction (R2p) of 0.95, and root mean square error of prediction (RMSEP) of 6.82%. The results indicate that NIR-HSI has the potential for detecting adulteration of powdered white pepper and can be successfully applied in food quality control for ensuring consumer confidence.

Keywords: *Adulteration, Classification, Prediction, Quality Control.*

1. Introduction

Food adulteration is primarily used to dilute the product stated on the label with a similar, cheaper product, mainly for economic reasons. However, it remains a serious global concern with significant implications for food safety, consumer health, and the economy. It has been reported that spices are among the various food products that are adulterated, particularly pepper [1, 2], with white pepper being popularly used for flavoring in many culinary dishes, especially in sauces, soups, and meat-based meals [3]. Substances that have been reported to be used to adulterate white paper include tapioca flour, corn flour, and mung bean flour [4-6]. Such fraudulent practices often compromise the quality of the spice and may also pose health risks, as some adulterants could introduce harmful substances [7] but adulterants may be difficult to detect.

Adulteration of white pepper with roasted rice, for example, is particularly challenging to detect due to the similarity in appearance and texture of the adulterant compared to genuine white pepper. Roasted rice is often used because it is cost-effective, readily available, and can easily mimic the ground form of white pepper. However, while both substances may appear similar under visual observation, their chemical compositions and spectral properties differ, making them detectable through advanced

History: Received: 3 October 2025; Revised: 19 November 2025; Accepted: 24 November 2025; Published: 1 January 2026
* Correspondence: sontisuk.te@kmitl.ac.th

technologies. This type of adulteration is especially concerning because it not only affects the sensory qualities of the product but also undermines consumer trust and market fairness [5].

The traditional methods of detecting food adulteration have relied heavily on physical inspection, chemical analysis, or microscopic techniques. However, these methods have limitations in terms of being time-consuming, costly, and using resources that could otherwise be sold. Observing physical properties through visual inspection may be difficult and can miss subtle traces of adulterants, while chemical analytical methods require sample preparation, chemical management, and complicated procedures. Microscopic techniques, although useful, are not always practical for large-scale or real-time applications. Therefore, there is an increasing demand for faster, more accurate, and non-destructive techniques to identify adulteration in food products [8, 9].

Near Infrared (NIR) spectroscopy is known as a powerful analytical tool that has been successfully used for detecting food adulteration by providing non-destructive and rapid results [10, 11]. NIR spectroscopy relies on the interaction of light, in the near-infrared spectrum, with the sample, providing information about its chemical composition based on the absorption of specific wavelengths of light. This method has been successfully applied in various fields, including the identification of food adulterants in oils, milk powder, butter, cheese, spices, paprika powder, and Sichuan pepper [12-17]. The successful use of NIR spectroscopy to detect adulterants, both qualitative and quantitative, has made it one of the most promising techniques for ensuring food authenticity [18].

A recent advance in NIR technology is hyperspectral imaging, which combines traditional NIR spectroscopy with spatial imaging. This method captures both the spectral and spatial information of a sample, allowing for detailed analysis of the sample's chemical composition and distribution [19, 20]. Hyperspectral imaging provides a comprehensive view of the sample, making it more sensitive and accurate in detecting adulterants even at low concentrations. The technique can detect variations in the chemical composition of both the adulterant and the food product, enabling the identification of even subtle differences [21]. This makes hyperspectral imaging particularly useful for detecting adulteration in food products, where adulterants are often mixed in small amounts to avoid detection [22]. Several studies have reported that NIR hyperspectral imaging (NIR-HSI) can be successfully used to detect adulteration in particulate food products, including peanut flour [23], tapioca starch [24], ground coffee [25], wheat flour [26, 27], chickpea flour [28], whey protein [29], Ceylon black tea [30], *Poria cocos* [31] and red pepper powder [32].

Additional advantages of hyperspectral imaging compared with traditional techniques include that it is a non-invasive method, which means it does not destroy samples, and also requires no chemical additives [33, 34]. Furthermore, hyperspectral imaging allows for real-time monitoring, making it possible to inspect large batches of food products quickly and efficiently [35]. These advantages make hyperspectral imaging particularly suitable for quality control in the food industry, where speed and accuracy are essential.

A further advantage for its application in commercial practice is that NIR hyperspectral imaging can be integrated with machine learning algorithms to enhance its detection capabilities. Machine learning models can be trained using spectral data from known samples to classify and predict the presence of adulterants in unknown samples. This integration of hyperspectral imaging and machine learning can significantly improve the reliability and accuracy of adulteration detection systems. By continuously refining these models with new data, the system can adapt to different types of adulteration, ensuring robustness in various real-world scenarios [36, 37].

The application of NIR hyperspectral imaging in food fraud detection not only benefits food safety but also contributes to the broader goal of transparency in the food supply chain. The ability of its application to verify the authenticity of food products enhances consumer confidence and helps maintain fair trade practices. As food fraud continues to increase, the use of innovative technologies like NIR

Edelweiss Applied Science and Technology
ISSN: 2576-8484
Vol. 10, No. 1: 1-15, 2026
DOI: 10.55214/2576-8484.v10i1.11489

hyperspectral imaging can play a critical role in safeguarding the integrity of the global food system [38].

The objective of this research was therefore to explore the use of NIR hyperspectral imaging in identifying adulterated white pepper powder mixed with roasted sticky rice powder, thus developing a robust classification model for distinguishing between pure white pepper powder and adulterated white pepper powder. A further aim of this study was to develop a reliable model for determining concentrations of roasted sticky rice powder in adulterated white pepper powder based on the correlation between spectral data and known concentrations of roasted sticky rice powder.

2. Materials and Methods

2.1. Sample Preparation

Dried white pepper (*Piper nigrum* L.) seeds and 'San Patong' sticky rice were purchased from a local market in Bangkok, Thailand. The white pepper seeds were ground by a grinder (Philips HR2223/00 Series 5000), and the acquired powder was screened through an 80-mesh sieve. Samples of the pure white pepper powder (N=100) were placed in zip-lock plastic bags and stored at 25 °C for the next step of the experiment. Sticky rice was roasted in a hot pan at 150 °C and stirred continuously until the color of the sticky rice changed to a golden yellow. The roasted sticky rice was ground using a grinder (Philips HR2223/00 Series 5000), and then the roasted sticky rice powder was screened using an 80-mesh sieve. Adulterated white pepper powder samples (N=118) were prepared by adding the roasted sticky rice powder into the white pepper powder, starting from 1% (weight/weight) and increasing by a similar interval until reaching 99% (weight/weight). All adulterated samples were well mixed and carefully placed in zip-lock plastic bags, and stored at 25 °C for further steps of the experiment.

2.2. Measurements of Properties

The appearance of the pure white pepper powder and the roasted sticky rice powder was visually similar; however, triplicate measurements for some properties of the pure white pepper powder and the roasted sticky rice powder, using randomly selected samples, were performed.

2.2.1. Color Measurement

The colors of pure white pepper powder and roasted sticky rice powder were measured by a colorimeter (Konica Minolta CR-400, Japan). L*, a*, b* color values, where L* indicates lightness (0 = black, 100 = white), a* represents the red/green (positive = red, negative = green), and b* represents the yellow/blue (positive = yellow, negative = blue), were acquired.

2.2.2. Protein Determination

The total nitrogen content of both the pure white pepper powder and the roasted sticky rice powder was measured using an automatic nitrogen analyzer (LECO FP528, Leco Corp., St. Joseph, MI, USA). The total protein content was determined using equation (1). The total protein content of pure white pepper powder was calculated by multiplying the nitrogen content by a conversion factor of 6.25, while the protein content of roasted sticky rice powder was calculated by multiplying the nitrogen content by a conversion factor of 5.95 [39].

$$\text{Protein (\%)} = \%\text{Nitrogen} \times \text{Conversion Factor} \quad (1)$$

2.2.3. Water Activity Measurement

The water activity (a_w) of both the pure white pepper powder and the roasted sticky rice powder was measured using a water activity meter (Lab Touch-aw, Novasina AG, Switzerland).

2.2.4. Moisture Content Determination

The moisture content of both the pure white pepper powder and the roasted sticky rice powder was determined following the AOAC official method [40] using a hot air oven (BINDER, FD 115, Germany). The moisture content was calculated by equation (2).

$$\text{Moisture (\%)} = \frac{(W_1 - W_2)}{W_1} \times 100 \quad (2)$$

where: W_1 = weight of sample before drying (g)
W_2 = weight of sample after drying (g)

2.3. NIR-HSI Measurement

The spectral information of each sample was acquired using a hyperspectral camera (Specim Fx17e, Spectral Imaging Ltd, Oulu, Finland) in the wavelength range from 935 nm to 1720 nm. The lamp consisted of six halogen lamps (three lamps on each side and 45° to the sample) with a scanning speed of 20 mm/s. A dark reference image was measured when the shutter was closed, and the camera was covered with a black lid. A white reference image was measured at every scan using a rectangular Spectralon bar.

2.4. Statistical Analysis

2.4.1 Principal Component Analysis (PCA)

PCA was applied as an unsupervised multivariate technique to reduce the dimensionality of the spectral data while preserving the maximum variance. This technique was used to transform correlated variables into a new set of principal components (PCs), enabling the visualization of patterns, group separation, and the detection of outliers. As reported by McKenzie et al. [41], PCA is widely used as a preliminary step prior to classification. In this study, the pure white pepper powder (N=100) and the roasted sticky rice powder (N=100) were analyzed using PCA.

2.4.2. Partial Least Squares (PLS)

PLS was employed as a supervised multivariate technique for both classification and quantitative prediction. Partial least squares discriminant analysis (PLS-DA) is an extension of PLS used to classify samples into categories [42]. While PLS regression (PLSR) was used to test the linear relationship between spectral data and dependent variables.

2.4.3. Support Vector Machine (SVM)

SVM is a powerful supervised machine learning technique widely used for classification and regression modeling. SVM operates by finding the optimal hyperplane that maximizes the margin between different classes in the feature space, making it especially suitable for handling high-dimensional, nonlinear, and complex datasets. Kernel functions are commonly employed to transform input data into a higher-dimensional space where linear separation is feasible [43].

2.5. Qualitative and quantitative analysis

2.5.1 Qualitative analysis

A total of 100 pure white pepper powder samples and 118 adulterated white pepper powder samples were analyzed using PLS-DA and support vector machine classification (SVMC) methods described above. For classification evaluation, the pure white pepper powder samples were labeled as 0, while the adulterated white pepper powder samples were labeled as 1. Samples were provided for both a calibration set and a prediction set. The spectral pretreatment methods, including smoothing, 1st derivative, 2nd derivative, MSC, SNV, and combined methods, were investigated using cross-validation

Edelweiss Applied Science and Technology
ISSN: 2576-8484
Vol. 10, No. 1: 1-15, 2026
DOI: 10.55214/2576-8484.v10i1.11489

of samples in the calibration set. This was done in order to select the best method for classification. The performance of the classification was evaluated using several key metrics: accuracy, error rate, sensitivity, and specificity [44] in order to provide a comprehensive evaluation of the classification capability in both the calibration and prediction sets.

In this case, accuracy was defined as the proportion of correctly classified samples (both true positives and true negatives) to the total number of samples. An accuracy value close to 100% implies a low error rate, indicating that the classification model performed well in classifying the samples correctly according to Equation (3):

$$Accuracy\ (\%) = \frac{(TP + TN)}{(TP + TN + FP + FN)} \times 100 \quad (3)$$

Error rate is the proportion of incorrectly classified samples presented in Equation (4):

$$Error\ rate\ (\%) = \frac{(FP + FN)}{(TP + TN + FP + FN)} \times 100 \quad (4)$$

Sensitivity (true positive rate) refers to the classification model's ability to correctly identify positive samples (adulterated white pepper powder) and was calculated as:

$$Sensitivity\ (\%) = \frac{TP}{(TP + FN)} \times 100 \quad (5)$$

Specificity (true negative rate) measures the accuracy of the classification model in correctly identifying negative samples (pure white pepper powder) and was calculated as:

$$Specificity\ (\%) = \frac{TN}{(TN + FP)} \times 100 \quad (6)$$

where TN is the true negative samples, TP is the true positive samples, FN is the false negative samples, and FP is the false positive samples.

2.5.2. Quantitative Analysis

A total of 122 samples, including adulterated white pepper powder samples (N=118), two pure white pepper powder samples, and two pure ground roasted rice samples, were used for the calibration and prediction sets. The calibration models were established using partial least squares regression (PLSR) and support vector machine regression (SVMR). The spectral pretreatment methods, including smoothing, first derivative, second derivative, multiplicative scatter correction (MSC), standard normal variate (SNV), and combined methods, were investigated using cross-validation of samples in the calibration set. This was done to select the best method for establishing the calibration model. The performance of the calibration models was determined using the coefficient of determination (R^2) and the root mean square error (RMSE), where high R^2 values and low RMSE (%) values in both the calibration and prediction sets indicated that the calibration model was accurate for predicting the level of roasted sticky rice powder in the adulterated white pepper powder.

The data were statistically analyzed using the SPSS software (version 24.0, IBM Corp., Armonk, NY, USA), the Unscrambler X software (version 10.4, CAMO Software AS, Oslo, Norway), and the Prediktera Evince software (version 2.7.9, Prediktera AB, Umea, Sweden).

3. Results and Discussion

3.1. Properties Comparison

The levels of L* and a* of the roasted sticky rice powder were both significantly higher ($p \leq 0.05$) than those of the pure white pepper powder, while the level of b* of the pure white pepper powder was significantly higher ($p \leq 0.05$) than that of the roasted sticky rice powder. The protein content of the pure white pepper powder was significantly higher than that of the roasted sticky rice powder ($p \leq 0.05$). In addition, the water activity and moisture content of the roasted sticky rice powder were significantly higher than those of the pure white pepper powder ($p \leq 0.05$) (Table 1). These findings

Edelweiss Applied Science and Technology
ISSN: 2576-8484
Vol. 10, No. 1: 1-15, 2026
DOI: 10.55214/2576-8484.v10i1.11489

indicate clear differences in the properties of the pure white pepper powder and the roasted sticky rice powder, although they are quite similar in visual appearance.

Table 1.
Properties of the pure white pepper powder and the roasted sticky rice powder.

Parameter		Pure White Pepper Powder	Roasted Sticky Rice Powder
Color	L*	66.47±0.28[a]	73.99±0.46[b]
	a*	1.16±0.65[a]	2.63±0.51[b]
	b*	24.61±1.20[a]	19.33±0.16[b]
Protein (%)		12.90±0.01[a]	7.54±0.06[b]
Water activity		0.04±0.00[a]	0.10±0.00[b]
Moisture content (%)		3.99±0.09[a]	4.58±0.09[b]

Note: Values are presented as mean ± standard deviation.
Different letters (a, b) in the same row of each parameter indicate significant differences ($p \leq 0.05$).

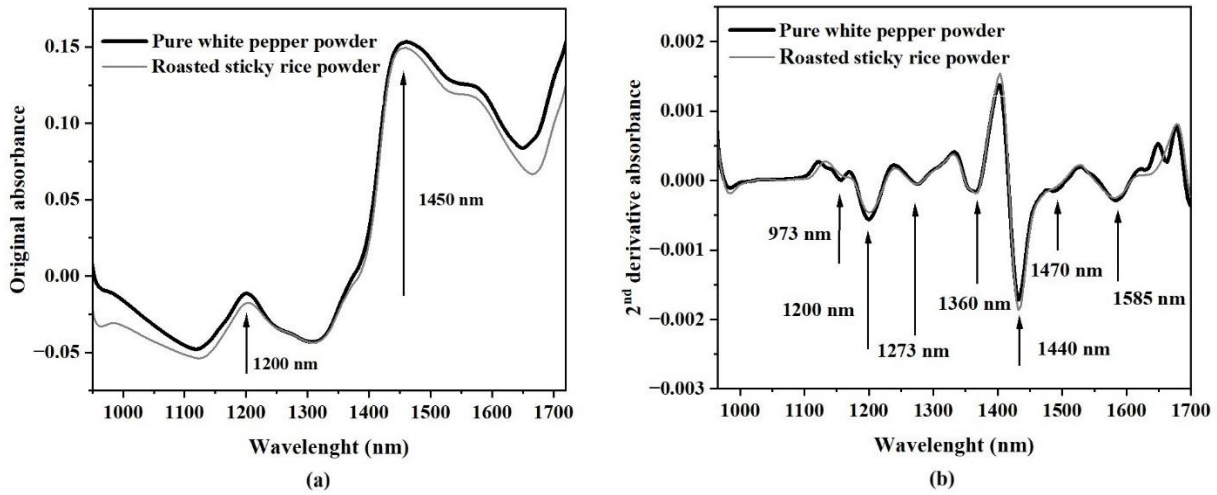

Figure 1.
The original absorbance spectra (a) and the 2nd derivative absorbance spectra (b) of the pure white pepper powder and the roasted sticky rice powder.

3.2. Spectral Characteristics

The absorbance peaks from the original spectra at around 1200 nm and 1450 nm (Figure 1) were associated with the characteristic absorption bands of water. These peaks correspond to the O–H bond in water molecules. Specifically, the 1200 nm peak corresponds to the second overtone of O–H stretching, while the 1450 nm peak is attributed to the first overtone of O–H stretching as described by Workman and Weyer [45] and Osborne and Fearn [46]. The 2nd derivative absorbance spectra showed peaks at 973, 1200, 1273, 1360, 1440, 1470, and 1585 nm, which are related to the chemical compositions of the pure white pepper powder and the roasted sticky rice powder (Figure 1b). The absorption band locations associated with proteins were at 973 nm, corresponding to N–H stretching second overtone, and at 1470 nm, corresponding to N–H stretching first overtone, as described by Workman and Weyer [45], and the water absorbance peak at 1200 nm was associated with the second overtone of the O–H stretching [45]. The absorbance peak observed at 1273 nm was related to the second overtone of C–H stretching, which corresponds to C–H functional groups [47]. The 1360 nm peak was linked to C–H combination bands, indicative of methyl groups (CH_3) [48]. The presence of

Edelweiss Applied Science and Technology
ISSN: 2576-8484
Vol. 10, No. 1: 1-15, 2026
DOI: 10.55214/2576-8484.v10i1.11489

sucrose and starch at the absorbance peak of 1440 nm was reported to be associated with the first overtone of O–H stretching [47], and the presence of starch and glucose molecules at the absorbance peak of 1585 nm was also attributed to the first overtone of O–H stretching [46].

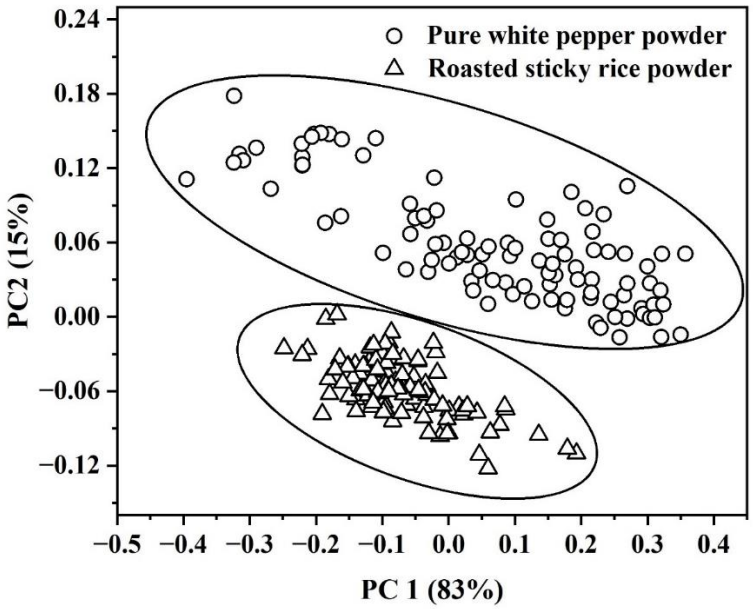

Figure 2.
PCA score plot of the pure white pepper powder and the roasted sticky rice powder.

The cumulative variance percentage was 98% from the two principal components (PC1 and PC2), with the variation for PC1 being 15% and for PC2 83% (Figure 2). This indicates that the two clusters of the pure white pepper powder and the roasted sticky rice powder were completely separated. This result clearly demonstrated that spectral data could be used to distinguish between pure tapioca starch and adulterated tapioca starch using this technique.

3.3. Acquisition from Qualitative Analysis

The characteristics of the samples used in the calibration and prediction sets for analysis were the same (Table 2).

Table 2.
The characteristics of samples in calibration and prediction sets for PLS-DA and SVMC.

Sets	Sample number	Minimum (%)	Maximum (%)	Mean (%)	Standard Deviation (%)
Calibration	152	0	1	0.54	0.05
Prediction	66	0	1	0.54	0.05

The PLS-DA results of accuracy, sensitivity, specificity, and error rate by cross-validation of samples in the calibration set (Figure 3a) showed that using original spectral data (non-pretreatment), using smoothing, and using 1st derivative spectral pretreatments achieved perfect classification performance, with 100% accuracy, sensitivity, and specificity without error rate. Therefore, the original spectral data were selected for classification by PLS-DA.

Edelweiss Applied Science and Technology
ISSN: 2576-8484
Vol. 10, No. 1: 1-15, 2026
DOI: 10.55214/2576-8484.v10i1.11489

The SVMC results for accuracy, sensitivity, specificity, and error rate, obtained through cross-validation of samples in the calibration set (Figure 3b), indicated that the combination of the 1st derivative with the SNV spectral pretreatment method provided the highest performance. It achieved 96.05% accuracy, 92.11% sensitivity, 100% specificity, and the lowest error rate of 3.95%. Therefore, the combination of the 1st derivative with the SNV spectral pretreatment method was selected for classification using SVMC.

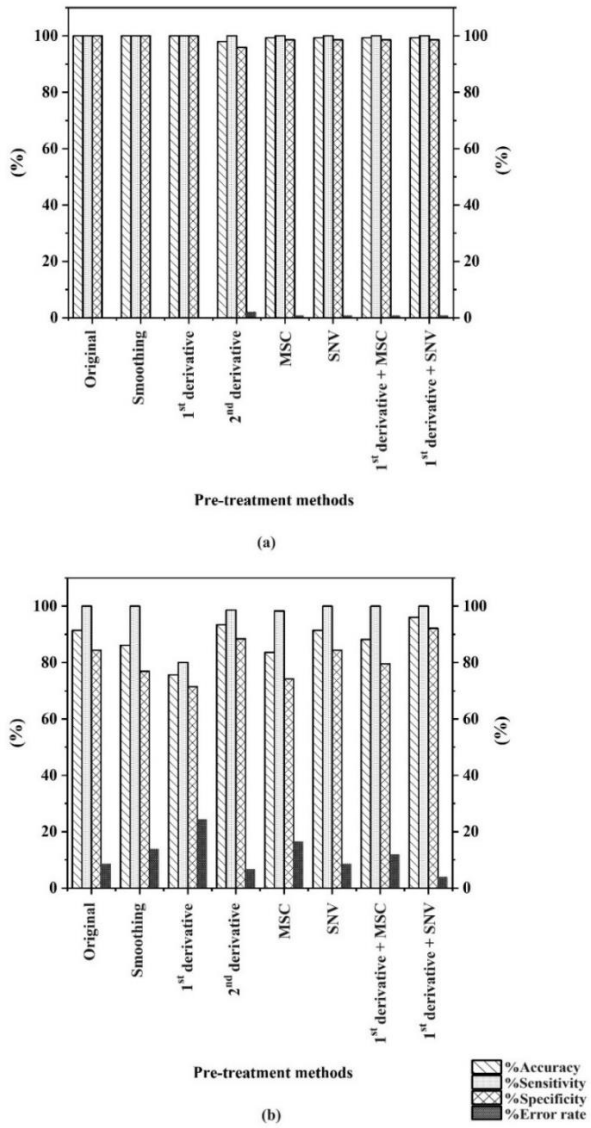

Figure 3.
Comparison of spectral pretreatment methods for classification in the calibration set using (a) PLS-DA and (b) SVMC.

Edelweiss Applied Science and Technology
ISSN: 2576-8484
Vol. 10, No. 1: 1-15, 2026
DOI: 10.55214/2576-8484.v10i1.11489

Table 3.
Performance of classification using PLS-DA and SVMC in the calibration set and the prediction set.

Methods	Pre-treatment	Factors		Data set	Pure white pepper powder (0)		Adulterated white pepper powder (1)		%Accuracy	%Sensitivity	%Specificity	%Error rate
					TRUE	FALSE	TRUE	FALSE				
PLS-DA	Original	8		Cal	70	0	82	0	100	100	100	0
				Pred	30		36	0	100	100	100	0
SVMC	1^{st} derivative + SNV	Nu	0.5	Cal	70	0	78	4	97.37	94.59	100	2.63
		γ	0.01	Pred	30		34	2	96.97	93.75	100	3.03

Note: PLS-DA = partial least squares discrimination analysis.
SVMC = support vector machine classification
SNV = standard normal variate
Cal = calibration set
Pred = prediction set
γ = kernel function parameter gamma
Nu = Nu parameter.

Edelweiss Applied Science and Technology
ISSN: 2576-8484
Vol. 10, No. 1: 1-15, 2026
DOI: 10.55214/2576-8484.v10i1.11489

The results of classification using PLS-DA and SVMC in the calibration set and the prediction set showed 100% accuracy, sensitivity, and specificity, without an error rate (%) in both sets, indicating that PLS-DA provided excellent performance for classification.

The combination of the 1st derivative with the SNV spectral pretreatment method was therefore selected for classifying pure white pepper powder and adulterated white pepper powder using SVMC with the Nu parameter of 0.5 and the kernel function parameter gamma (γ) of 0.01. The classification results showed 97.37% accuracy, 94.59% sensitivity, 100% specificity, and a 2.63% error rate in the calibration set, and 96.97% accuracy, 93.75% sensitivity, 100% specificity, and a 3.03% error rate in the prediction set. These results indicate that SVMC provided good performance for classification (Table 3). From these results, it was shown that PLS-DA was more effective for differentiating between the pure white pepper powder and the adulterated white pepper powder than SVMC.

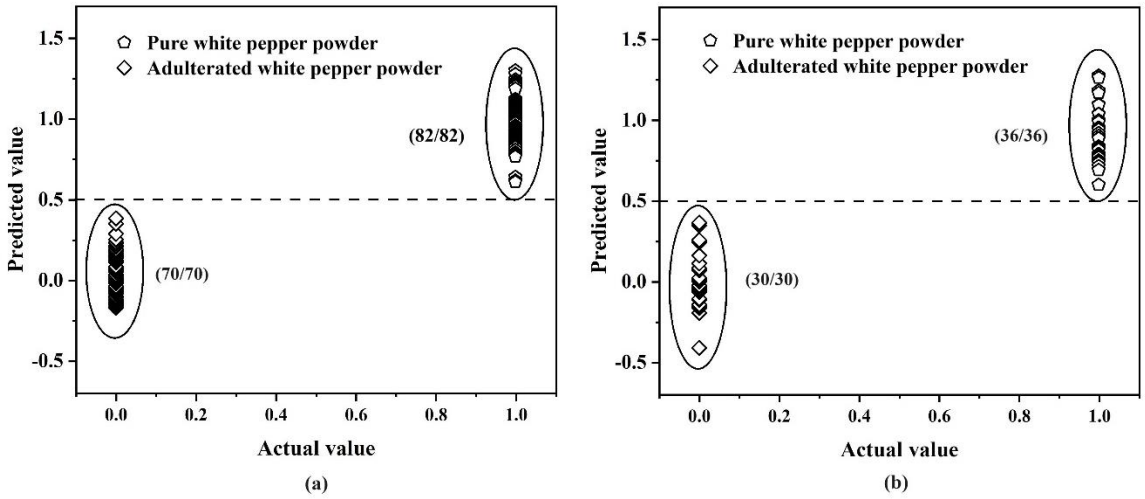

Figure 4.
The classification for the pure white pepper powder samples (0) and the adulterated white pepper powder samples (1) using PLS-DA in both the calibration set (a) and the prediction set (b).

The scatter plots of classification between the pure white pepper powder samples (0) and the adulterated white pepper powder samples (1) using PLS-DA are shown in Figure 4. The cutoff value of 0.5 was used for classification. If the predicted value of each sample was equal to or less than 0.5, it was classified as a pure white pepper powder sample, while if the predicted value was higher than 0.5, it was classified as an adulterated white pepper powder sample. The results demonstrated that PLS-DA, when using the original spectral data of samples, achieved perfect classification in both the calibration and prediction sets.

3.4. Acquisition from Quantitative Analysis

Both the calibration set (N=85) and the prediction set (N=37) for quantitative analysis using PLSR and SVMR contained samples characterized by the level of roasted sticky rice powder in the adulterated white pepper powder. The characteristics of these samples in both the calibration and prediction sets exhibited a well-distribution of data, as evidenced by their similar mean and standard deviation values (Table 4).

Edelweiss Applied Science and Technology
ISSN: 2576-8484
Vol. 10, No. 1: 1-15, 2026
DOI: 10.55214/2576-8484.v10i1.11489

Table 4.
The characteristics of the level of the roasted sticky rice powder in the adulterated white pepper powder of samples in the calibration and prediction sets.

Sets	Sample number	Minimum (%)	Maximum (%)	Mean (%)	Standard Deviation (%)
Calibration	85	0	100	49.83	29.26
Prediction	37	1	98	50.16	30.41

The various spectral pretreatment methods for PLSR results by cross-validation showed that MSC spectral pretreatment obtained the best performance of the calibration model, with the highest R^2_{cv} of 0.88 and the lowest RMSECV of 10.46%. (Figure 5a). Therefore, MSC spectral pretreatment was selected for creating the PLSR model. Additionally, the SVMR results by cross-validation indicated that SNV spectral pretreatment provided the best performance of the calibration model, with the highest R^2_{cv} of 0.95 and the lowest RMSECV of 7.54%. (Figure 5b). Consequently, SNV spectral pretreatment was chosen for developing the SVMR model in this study.

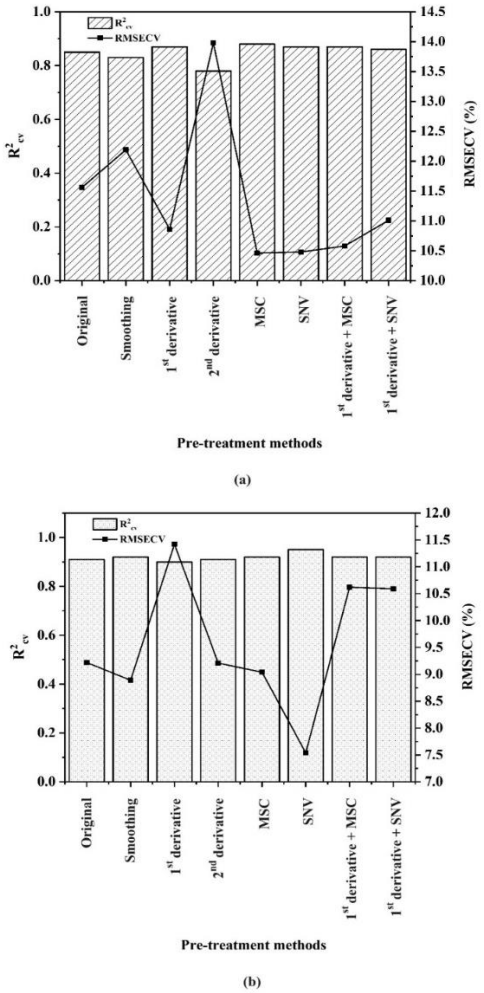

Figure 5.
Spectral pretreatment methods for establishing the PLSR model (a) and the SVMR model (b).

Edelweiss Applied Science and Technology
ISSN: 2576-8484
Vol. 10, No. 1: 1-15, 2026
DOI: 10.55214/2576-8484.v10i1.11489

Table 5.
Performance of the PLSR model and the SVMR model in the calibration set and the prediction set.

Methods	Pre-treatment	Factors		R^2_c	R^2_p	RMSEC (%)	RMSEP (%)
PLSR	MSC	1		0.88	0.88	10.15	10.12
SVMR	SNV	c	γ	0.96	0.95	6.49	6.82
		0.1	0.01				

Note: PLSR = partial least squares regression
SVMR = support vector machine regression
MSC = multiplicative scatter correction
SNV = standard normal variate
R^2_c = coefficient of determination of calibration
RMSEC = root mean square error of calibration
R^2_p = coefficient of determination of prediction
RMSEP = root mean square error of prediction
c = penalty factor
γ = kernel function parameter gamma.

The PLSR model, developed using MSC spectral pretreatment, yielded an R^2_p of 0.88 and an RMSEP of 10.12%. In contrast, the SVMR model, developed using SNV spectral pretreatment, achieved an R^2_p of 0.95 and an RMSEP of 6.82%. Therefore, the SVMR model was demonstrated to be more accurate in determining the level of roasted sticky rice powder in adulterated white pepper powder (Table 5).

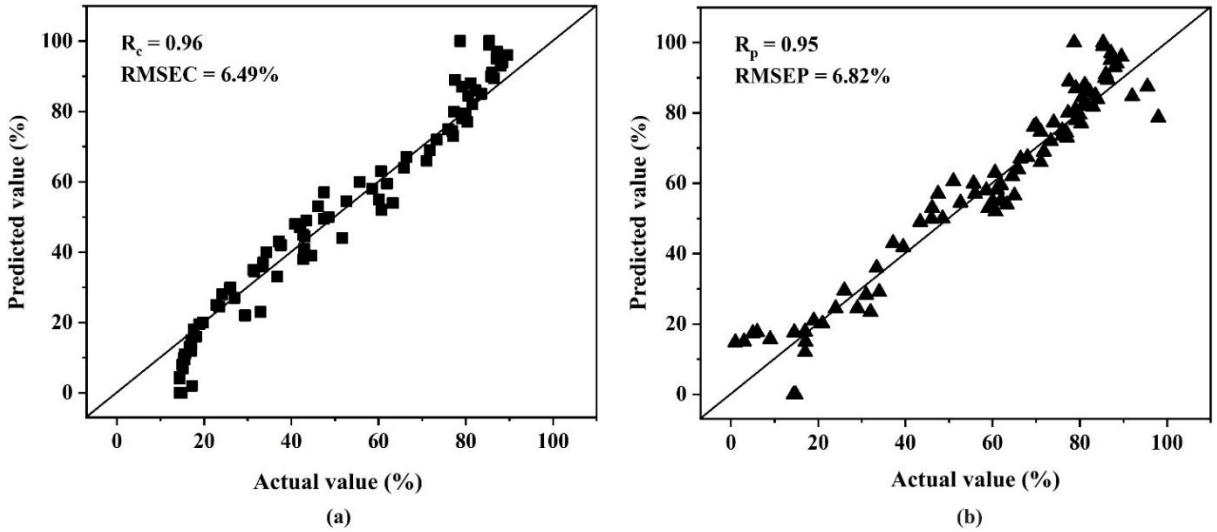

Figure 6.
The scatter plots of the actual value and the predicted value of the level of roasted sticky rice powder in adulterated white pepper powder using the SVMR model in the calibration set (a) and the prediction set (b).

The performance of the data from the SVMR model closely aligned along the 45-degree reference line, indicating a strong agreement between the predicted and actual values (Figures 6a and 6b). Confirming that the SVMR model provided accurate quantitative predictions of the level of roasted sticky rice powder in the adulterated white pepper powder.

Edelweiss Applied Science and Technology
ISSN: 2576-8484
Vol. 10, No. 1: 1-15, 2026
DOI: 10.55214/2576-8484.v10i1.11489

4. Conclusions

From this study, it was shown that near-infrared hyperspectral imaging has the potential to be used for identifying when white pepper powder has been contaminated with roasted rice powder. It also demonstrated its potential for identifying the actual level of adulteration. It was shown that using partial least squares discriminant analysis resulted in 100% accuracy. Additionally, support vector machine regression and standard normal variate enhancement improved the predictive performance for determining the concentration of roasted sticky rice powder in adulterated white pepper powder. These findings indicate that near-infrared hyperspectral imaging could be used to establish a reliable model for identifying adulteration of white pepper powder in real-time. This method is fast, reliable, and applicable in a non-destructive manner in a commercial setting.

Funding:

This work was financially supported by King Mongkut's Institute of Technology, Ladkrabang Research Fund (Grant Number: RE-KRIS/FF67/064).

Transparency:

The authors confirm that the manuscript is an honest, accurate, and transparent account of the study; that no vital features of the study have been omitted; and that any discrepancies from the study as planned have been explained. This study followed all ethical practices during writing.

Acknowledgments:

The authors would like to thank King Mongkut's Institute of Technology, Ladkrabang, for its financial support and Professor Dr. Panmanas Sirisomboon for valuable technical assistance.

References

[1] P. Galvin-King, S. A. Haughey, and C. T. Elliott, "Herb and spice fraud; the drivers, challenges and detection," *Food Control*, vol. 88, pp. 85-97, 2018. https://doi.org/10.1016/j.foodcont.2017.12.031

[2] J. P. Sahoo and K. C. Sama, "Adulteration in Indian spices: An alarming concern and a silent health hazard," *International Journal of Adulteration*, vol. 8, no. 9, pp. 1–9, 2024. https://doi.org/10.54905/disssi.v8i9.e4ijad3043

[3] C. Spence, "The king of spices: On pepper's pungent pleasure," *International Journal of Gastronomy and Food Science*, vol. 35, p. 100900, 2024. https://doi.org/10.1016/j.ijgfs.2024.100900

[4] A. Sarifudin *et al.*, "Adulterated powdered white pepper products by tapioca flour sold in Indonesian's online market investigated by simple FTIR analytical method," *Journal of Food and Nutrition Research*, vol. 9, no. 6, pp. 297-303, 2021. https://doi.org/10.12691/jfnr-9-6-5

[5] R. Chen, J. Mei, G. Du, Y. Shi, and Y. Huang, "Convenient detection of white pepper adulteration by portable NIRS and spectral imaging with chemometrics," *Microchemical Journal*, vol. 182, p. 107925, 2022. https://doi.org/10.1016/j.microc.2022.107925

[6] Y. P. Sari, A. R. Putri, S. T. C. Murti, A. Setiyoko, and T. E. Purbaningtias, "Fast detection of white pepper adulteration using FTIR-ATR spectroscopy and chemometrics," *Malaysian Journal of Science and Advanced Technology*, vol. 5, no. 1, pp. 66-71, 2025. https://doi.org/10.56532/mjsat.v5i1.426

[7] Y. K. Anagaw *et al.*, "Food adulteration: Causes, risks, and detection techniques," *SAGE Open Medicine*, vol. 12, p. 20503121241250184, 2024. https://doi.org/10.1177/20503121241250184

[8] R. Goyal, P. Singha, and S. K. Singh, "Spectroscopic food adulteration detection using machine learning: Current challenges and future prospects," *Trends in Food Science & Technology*, vol. 146, p. 104377, 2024. https://doi.org/10.1016/j.tifs.2024.104377

[9] M. H. Nargesi, J. Amiriparian, H. Bagherpour, and K. Kheiralipour, "Detection of different adulteration in cinnamon powder using hyperspectral imaging and artificial neural network method," *Results in Chemistry*, vol. 9, p. 101644, 2024. https://doi.org/10.1016/j.rechem.2024.101644

[10] J.-H. Qu *et al.*, "Applications of near-infrared spectroscopy in food safety evaluation and control: A review of recent research advances," *Critical Reviews in Food Science and Nutrition*, vol. 55, no. 13, pp. 1939-1954, 2015. https://doi.org/10.1080/10408398.2013.871693

[11] E. Shawky, L. Nahar, S. M. Nassief, S. D. Sarker, and R. S. Ibrahim, "Spice authentication by near-infrared spectroscopy: Current advances, limitations, and future perspectives," *Trends in Food Science & Technology*, vol. 148, p. 104522, 2024. https://doi.org/10.1016/j.tifs.2024.104522

[12] N. Vanstone, A. Moore, P. Martos, and S. Neethirajan, "Detection of the adulteration of extra virgin olive oil by near-infrared spectroscopy and chemometric techniques," *Food Quality and Safety*, vol. 2, no. 4, pp. 189-198, 2018. https://doi.org/10.1093/fqsafe/fyy018

[13] L. Cai, Y. Zheng, Y. Liu, R. Zhou, and M. Ma, "Near-infrared (NIR) spectroscopy combined with chemometrics for qualitative and quantitative detection of camel milk powder adulteration," *Journal of Food Composition and Analysis*, vol. 143, p. 107571, 2025. https://doi.org/10.1016/j.jfca.2025.107571

[14] M. L. da Silva Medeiros, A. F. Lima, M. C. Goncalves, H. T. Godoy, and D. F. Barbin, "Portable near-infrared (NIR) spectrometer and chemometrics for rapid identification of butter cheese adulteration," *Food Chemistry*, vol. 425, p. 136461, 2023. https://doi.org/10.1016/j.foodchem.2023.136461

[15] M. M. Oliveira, J. Cruz-Tirado, and D. F. Barbin, "Nontargeted analytical methods as a powerful tool for the authentication of spices and herbs: A review," *Comprehensive Reviews in Food Science and Food Safety*, vol. 18, no. 3, pp. 670-689, 2019. https://doi.org/10.1111/1541-4337.12436

[16] M. Oliveira, J. Cruz-Tirado, J. Roque, R. Teófilo, and D. Barbin, "Portable near-infrared spectroscopy for rapid authentication of adulterated paprika powder," *Journal of Food Composition and Analysis*, vol. 87, p. 103403, 2020. https://doi.org/10.1016/j.jfca.2019.103403

[17] X.-Y. Wu, S.-P. Zhu, H. Huang, and D. Xu, "Quantitative identification of adulterated sichuan pepper powder by near-infrared spectroscopy coupled with chemometrics," *Journal of Food Quality*, vol. 2017, no. 1, p. 5019816, 2017. https://doi.org/10.1155/2017/5019816

[18] P. F. Ndlovu, L. S. Magwaza, S. Z. Tesfay, and R. R. Mphahlele, "Destructive and rapid non-invasive methods used to detect adulteration of dried powdered horticultural products: A review," *Food Research International*, vol. 157, p. 111198, 2022. https://doi.org/10.1016/j.foodres.2022.111198

[19] C. B. Karaziack, C. Vidal, C. Pasquini, D. F. Barbin, and W. H. Viotto, "Application of near-infrared hyperspectral imaging for determination of cheese chemical composition," *Journal of Food Composition and Analysis*, vol. 127, p. 105994, 2024. https://doi.org/10.1016/j.jfca.2024.105994

[20] Y.-H. Miao, L.-Y. Zong, and W.-H. Su, "Machine learning in point spectroscopy and hyperspectral imaging for rapid detection of staple foods quality and safety: A review," *Journal of Food Composition and Analysis*, vol. 148, p. 108422, 2025. https://doi.org/10.1016/j.jfca.2025.108422

[21] H. T. Temiz and B. Ulaş, "A review of recent studies employing hyperspectral imaging for the determination of food adulteration," *Photochem*, vol. 1, no. 2, pp. 125-146, 2021. https://doi.org/10.3390/photochem1020008

[22] X. Zhao, W. Wang, X. Ni, X. Chu, Y.-F. Li, and C. Lu, "Utilising near-infrared hyperspectral imaging to detect low-level peanut powder contamination of whole wheat flour," *Biosystems Engineering*, vol. 184, pp. 55-68, 2019. https://doi.org/10.1016/j.biosystemseng.2019.06.010

[23] A. Laborde, F. Puig-Castellví, D. J.-R. Bouveresse, L. Eveleigh, C. Cordella, and B. Jaillais, "Detection of chocolate powder adulteration with peanut using near-infrared hyperspectral imaging and Multivariate Curve Resolution," *Food Control*, vol. 119, p. 107454, 2021. https://doi.org/10.1016/j.foodcont.2020.107454

[24] D. Khamsopha, S. Woranitta, and S. Teerachaichayut, "Utilizing near infrared hyperspectral imaging for quantitatively predicting adulteration in tapioca starch," *Food Control*, vol. 123, p. 107781, 2021. https://doi.org/10.1016/j.foodcont.2020.107781

[25] W. Sahachairungrueng, C. Meechan, N. Veerachat, A. K. Thompson, and S. Teerachaichayut, "Assessing the levels of robusta and arabica in roasted ground coffee using NIR hyperspectral imaging and FTIR spectroscopy," *Foods*, vol. 11, no. 19, p. 3122, 2022. https://doi.org/10.3390/foods11193122

[26] L. Zheng *et al.*, "Determination of adulteration in wheat flour using multi-grained cascade forest-related models coupled with the fusion information of hyperspectral imaging," *Spectrochimica Acta Part A: Molecular and Biomolecular Spectroscopy*, vol. 270, p. 120813, 2022. https://doi.org/10.1016/j.saa.2021.120813

[27] H.-J. He, Y. Chen, G. Li, Y. Wang, X. Ou, and J. Guo, "Hyperspectral imaging combined with chemometrics for rapid detection of talcum powder adulterated in wheat flour," *Food Control*, vol. 144, p. 109378, 2023. https://doi.org/10.1016/j.foodcont.2022.109378

[28] D. Saha, T. Senthilkumar, C. B. Singh, and A. Manickavasagan, "Quantitative detection of metanil yellow adulteration in chickpea flour using line-scan near-infrared hyperspectral imaging with partial least square regression

and one-dimensional convolutional neural network," *Journal of Food Composition and Analysis*, vol. 120, p. 105290, 2023. https://doi.org/10.1016/j.jfca.2023.105290

[29] W. Song *et al.*, "Authentication and quality assessment of whey protein-based sports supplements using portable near-infrared spectroscopy and hyperspectral imaging," *Food Research International*, vol. 203, p. 115807, 2025. https://doi.org/10.1016/j.foodres.2025.115807

[30] A. Menevseoglu, N. Gunes, E. Agcam, S. S. Turgut, and D. Pérez-Marín, "Comprehensive chemometric and machine learning methods for determination of synthetic dyes adulteration in ceylon tea via NIR spectroscopy and hyperspectral imaging," *Microchemical Journal*, vol. 218, p. 115697, 2025. https://doi.org/10.1016/j.microc.2025.115697

[31] M. Luan *et al.*, "Hyperspectral Imaging Combined with Chemometrics for Rapid Detection of Poria cocos Adulteration: A Qualitative and Quantitative Approach," *Journal of Food Composition and Analysis*, vol. 145, p. 107835, 2025. https://doi.org/10.1016/j.jfca.2025.107835

[32] G.-U. Seong *et al.*, "Characterization of bioactive compounds in phytophthora blight-infected red pepper powder (Capsicum annuum) and nondestructive discrimination of adulteration ratios using hyperspectral imaging," *Food Bioscience*, vol. 63, p. 105662, 2025. https://doi.org/10.1016/j.fbio.2024.105662

[33] G. Özdoğan, X. Lin, and D.-W. Sun, "Rapid and noninvasive sensory analyses of food products by hyperspectral imaging: Recent application developments," *Trends in Food Science & Technology*, vol. 111, pp. 151-165, 2021. https://doi.org/10.1016/j.tifs.2021.02.044

[34] M. Medina–García, J. M. Amigo, M. A. Martínez-Domingo, E. M. Valero, and A. M. Jiménez–Carvelo, "Strategies for analysing hyperspectral imaging data for food quality and safety issues–A critical review of the last 5 years," *Microchemical Journal*, vol. 214, p. 113994, 2025. https://doi.org/10.1016/j.microc.2025.113994

[35] Z. Kang, Y. Zhao, L. Chen, Y. Guo, Q. Mu, and S. Wang, "Advances in machine learning and hyperspectral imaging in the food supply chain," *Food Engineering Reviews*, vol. 14, pp. 596-616, 2022. https://doi.org/10.1007/s12393-022-09322-2

[36] M. Nikzadfar *et al.*, "Hyperspectral imaging aiding artificial intelligence: A reliable approach for food qualification and safety," *Applied Sciences*, vol. 14, no. 21, p. 9821, 2024. https://doi.org/10.3390/app14219821

[37] M.-F. Cheng, A. Mukundan, R. Karmakar, M. A. E. Valappil, J. Jouhar, and H.-C. Wang, "Modern trends and recent applications of hyperspectral imaging: A review," *Technologies*, vol. 13, no. 5, p. 170, 2025. https://doi.org/10.3390/technologies13050170

[38] J. Mendez, L. Mendoza, J. Cruz-Tirado, R. Quevedo, and R. Siche, "Trends in application of NIR and hyperspectral imaging for food authentication," *Scientia Agropecuaria*, vol. 10, no. 1, pp. 143-161, 2019. http://dx.doi.org/10.17268/sci.agropecu.2018.01.16

[39] A. Ndiaye, A. Traore, P. S. Gueye, Z. Senwo, M. Ndiaye, and A. Diop, "Metal and pesticide assessments of imported and locally cultivated rice (Oryza sativa) in Senegal," *Applied Sciences*, vol. 14, no. 7, p. 2876, 2024. https://doi.org/10.3390/app14072876

[40] AOAC, *Official methods of analysis*, 17th ed. Gaithersburg, MD, USA: Assoc. Off. Anal. Chemists, 2000.

[41] J. S. McKenzie, J. A. Donarski, J. C. Wilson, and A. J. Charlton, "Analysis of complex mixtures using high-resolution nuclear magnetic resonance spectroscopy and chemometrics," *Progress in Nuclear Magnetic Resonance Spectroscopy*, vol. 59, no. 4, pp. 336-359, 2011. https://doi.org/10.1016/j.pnmrs.2011.04.003

[42] L. C. Lee, C.-Y. Liong, and A. A. Jemain, "Partial least squares-discriminant analysis (PLS-DA) for classification of high-dimensional (HD) data: a review of contemporary practice strategies and knowledge gaps," *Analyst*, vol. 143, no. 15, pp. 3526-3539, 2018. https://doi.org/10.1039/C8AN00599K

[43] V. Vapnik, *The nature of statistical learning theory*, 2nd ed. New York, USA: Springer, 2000.

[44] M. Sokolova and G. Lapalme, "A systematic analysis of performance measures for classification tasks," *Information Processing & Management*, vol. 45, no. 4, pp. 427-437, 2009. https://doi.org/10.1016/j.ipm.2009.03.002

[45] J. Workman and L. Weyer, *Practical guide and spectral atlas for interpretive near-infrared spectroscopy*, 2nd ed. Boca Raton, FL, USA: Taylor & Francis Group, 2012.

[46] B. G. Osborne and T. Fearn, *Near infrared spectroscopy in food analysis*. London, U.K: Longman Scientific & Technical, 1986.

[47] C. Dachoupakan Sirisomboon, P. Wongthip, and P. Sirisomboon, "Potential of near infrared spectroscopy as a rapid method to detect aflatoxins in brown rice," *Journal of Near Infrared Spectroscopy*, vol. 27, no. 3, pp. 232-240, 2019. https://doi.org/10.1177/0967033519835051

[48] H. P. R. Aenugu, D. S. Kumar, N. P. Srisudharson, S. Ghosh, and D. Banji, "Near infra red spectroscopy—An overview," *International Journal of ChemTech Research*, vol. 3, no. 2, pp. 825-836, 2011.